Journal of the Serbian Chemical Society
JSCS-info@shd.org.rs • www.shd.org.rs/JSCS

J. Serb. Chem. Soc. 85 (5) 651–660 (2020)
JSCS–5328

Original scientific paper

Decomposition mechanism of dihydroxylammonium 5,5'-bis(tetrazole)-1,1'-diolate on Al(111) surface by periodic DFT calculation

YING ZHAO[1], XIAOLING XING[2], SHENGXIANG ZHAO[2] and XUEHAI JU[1]*

[1]*School of Chemical Engineering, Nanjing University of Science and Technology, Nanjing 210094, P. R. China and* [2]*Xi'an Modern Chemistry Research Institute, Xi'an 710065, P. R. China*

(Received 28 August, revised 1 November, accepted 27 November 2019)

Abstract: The generalized gradient approximation (GGA) of density function theory (DFT) methods are employed to investigate the decomposition of TKX--50 molecule on the Al(111) surface. The calculation employs an Al supercell slab model and periodic boundary conditions. Five kinds of adsorption configurations for TKX-50 on Al surface are studied. The TKX-50 is adsorbed on Al surface to form the N–Al, O–Al and OH–Al bonds. The adsorption energies are in the range from –113.15 to –1334.40 kJ/mol. The activation energies of all configurations are in the range of 100.34–354.10 kJ/mol. The N_1-N_2 ruptures in V1 and N_2-N_3 ruptures in V2 takes place easily. The activation energies of these two bonds rupture (100.34 and 108.06 kJ/mol, respectively) are less than that of pure TKX-50 (161.58 and 215.99 kJ/mol). Al atoms promote the breaking of the tetrazole ring of TKX-50. The quantities of electron transfer from Al atoms to TKX-50 are in range of 1.42–4.90 e.

Keywords: TKX-50; adsorption; transient states; activation energy; charge transfer.

INTRODUCTION

Aluminum, as a kind of active metal, is widely used in the energetic materials (EMs) because of its excellent combustion performance. In the development and application of propellants, adding appropriate amount of aluminum powder to the propellant may efficiently improve its exothermic property of combustion, burning rate and impact effect.[1–3] The effects, mentioned above, depend on the size of Al particles. The smaller the Al particles, the more obvious the improvement of explosive performance. Some researchers indicated that the Al nanopowder with high surface area can enhance the performance of EMs.[4]

* Corresponding author. E-mail: xhju@njust.edu.cn
https://doi.org/10.2298/JSC190828127Z

TKX-50, chemical name of dihydroxylammonium 5,5'-bis(tetrazole)-1,1'--diolate, is a newly synthesized nitrogen-rich energetic salt.[5] TKX-50 possesses broad application prospects in EMs on account of its outstanding performance: high energy storage, low impact, sensitivity and low toxicity.[6] Hence, TKX-50 may substitute some traditional explosives in propellants. Also, KX-50 thermal decompositions of both gaseous and solid-phase have been investigated experimentally and theoretically. For instance, An *et al.*, based on the quantum calculations,[7] have found that the initial thermal decomposition of TKX-50 involves ring breaking to release nitrogen. Yuan *et al.* concluded that nitrogen products are released by the ring opening of the tetrazole of TKX-50 in its excited state.[8] Wang *et al.* for the first time proved that diammonium 5,5'-bistetrazole-1,1'-diolate is the primary decomposition product of TKX-50.[9] However, the decomposition of TKX-50 on Al surface is not jet completely clarified. The Al(111) surface is known as easily exposed and easily oxidized.[10,11] Hence, we studied the interaction mechanism between the energetic compound of TKX-50 and the Al(111) surface theoretically. Five kinds of adsorption and decomposition configurations of TKX-50 on Al(111) surface were investigated. The stable geometries and energies in the adsorption and decomposition process, as well as the electron transfer were analyzed.

COMPUTATIONAL METHODS

The CASTEP module of Materials Studio 7.0 was employed to perform all the calculations.[12] The density functional theory methods are used widely to calculate the surface interaction.[13-15] The DFT methods are suitable way to study the adsorption behavior of molecule on surface.[16-20] The wave function of calculation is based on the Vanderbilt-type ultrasoft pseudopotentials and a plane-wave expansion.[21] Exchange and correlation were treated with the generalized gradient approximation (GGA). Compared with the local density approximation (LDA), GGA can take into account the non-uniformity of electron density in the real system. But LDA uses a uniform electron gas model. It can be used to describe a system in which the electron density does not change very much in space. Hence, in the calculation results of LDA there are serious errors for systems with fewer electrons such as transition state in a chemical reaction and in the calculation of binding energy. However, GGA can describe appropriately this system mentioned above since it consider the density gradient. The functional form of Perdew, Burke and Ernzerh (PBE) and a density-mixing scheme are used to obtain the electronic wave functions.[22-23] The Broyden, Fletcher, Goldfarb and Shannon (BFGS) methods were used to relax the structures.[24] The cutoff energy of plane waves was set to be 340 eV. The Monkhost–Pack scheme was used to perform Brillouin zone sampling. The grid parameters of k-point are set as 3×3×3. The value of kinetic energy cutoff and the k-point grid ensure the convergence of total energies.

A slab model with periodic boundary conditions represents the Al surface (Fig. 1). In view of the balance of both computational efficiency and precision, a 4×5 supercell with three layers containing 60 Al atoms was constructed to study the decomposition process of TKX-50 molecule on the Al(111) surface. The slabs were separated by 16 Å of vacuum along the

c-axis direction with a TKX-50 molecules on the top of the slab. The lattice parameters of *a*×*b*×*c* are 11.43×14.29×20.67 Å.

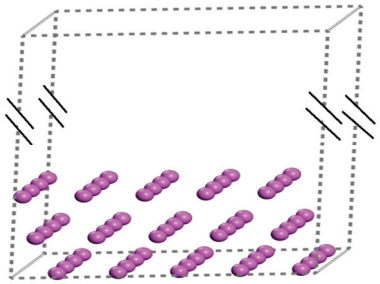

Fig. 1. Model of Al(111) slab (16 Å of vacuum above Al slab).

In order to confirm the accuracy of the calculation method, the functionals form of PBE, Perdew–Wang 91 (PW91), revised PBE (RPBE) and Wu–Cohen (WC) were used to optimize the isolated TKX-50 molecule in a box with dimensions of 11.43×14.29×20.67 Å and Al cell. Therein, the Al original cell is obtained from COD database. The equilibrium structure parameters calculated by these four functionals are compared with the experiment data. Tables S-I and S-II of the Supplementary material to this paper present the equilibrium structure parameters of TKX-50 and Al cell, respectively. It can be observed that the structure parameters calculated by PBE functional are closest to the experimental data. For instance, the calculation results show that the optimized crystal cell parameters are 4.058×4.058×4.058 Å. The computational lattice constants are close to the experimental values (4.050×4.050×4.050 Å), indicating that the present method can simulate the structural properties of bulk aluminum properly. These tests also verify the accuracy of the calculation method for the adsorption between TKX-50 molecules and Al (111) surface, such as the optimum cutoff energy and k-points for calculations. The good agreement between simulation results of aluminum and the TKX-50 molecule with the experiment suggest that the computation method is suitable for the simulation of TKX-50 molecular adsorption and decomposition behavior on the Al(111) surface.

For the adsorption configurations, the adsorption energy (E_{ad}) was calculated according to the equation:

$$E_{ad} = E_{(adsorbate + salb)} - E_{(molecule + slab)} \quad (1)$$

where $E_{(adsorbate + salb)}$ is the total energy of the adsorbate/Al-slab system after TKX-50 molecule absorbed onto the Al-slab; $E_{(molecule + slab)}$ is the single-point energy of the TKX-50/Al--slab system but without interactions between TKX-50 molecule and the Al-slab surface.

The LST/QST method was used to search the transition states (TS). Firstly, the liner synchronous transit (LST) maximization was performed, then the energy along the reaction pathway was minimized. The quadratic synchronous transit (QST) maximization was performed by the TS approximation obtained in that way. Another conjugate gradient minimization was performed from the point. The cycle was repeated until a stationary point was located.[25-29] The convergence criterion of the transition state calculations was set to 0.25 eV/Å for the root mean-square force. The activation energy is defined as:

$$E_a = E_{TS} - E_R \quad (2)$$

where E_{TS} is the energy of transition state, E_R is the sum of energies of reactants.

RESULTS AND DISCUSSION

Decomposition configuration and adsorption energy

On the basis of the initial orientation of tetrazole ring of TKX-50 relative to the Al(111) surface, five types of configurations (**P**, **T1**, **T2**, **V1** and **V2**) are defined. **P** is a parallel to the Al(111) surface, **T1** and **T2** are tilt, **V1** and **V2** are vertical. The structure of TKX-50 and its atomic number are given in Fig. 2. The adsorption configurations of decomposed TKX-50 molecule are shown in Fig. 3. Table I presents the adsorption energies calculated by Eq. (1).

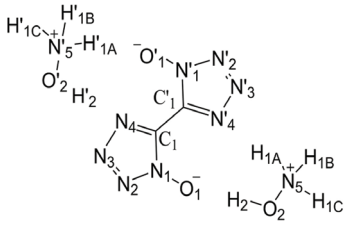

Fig. 2. Molecular structure of TKX-50.

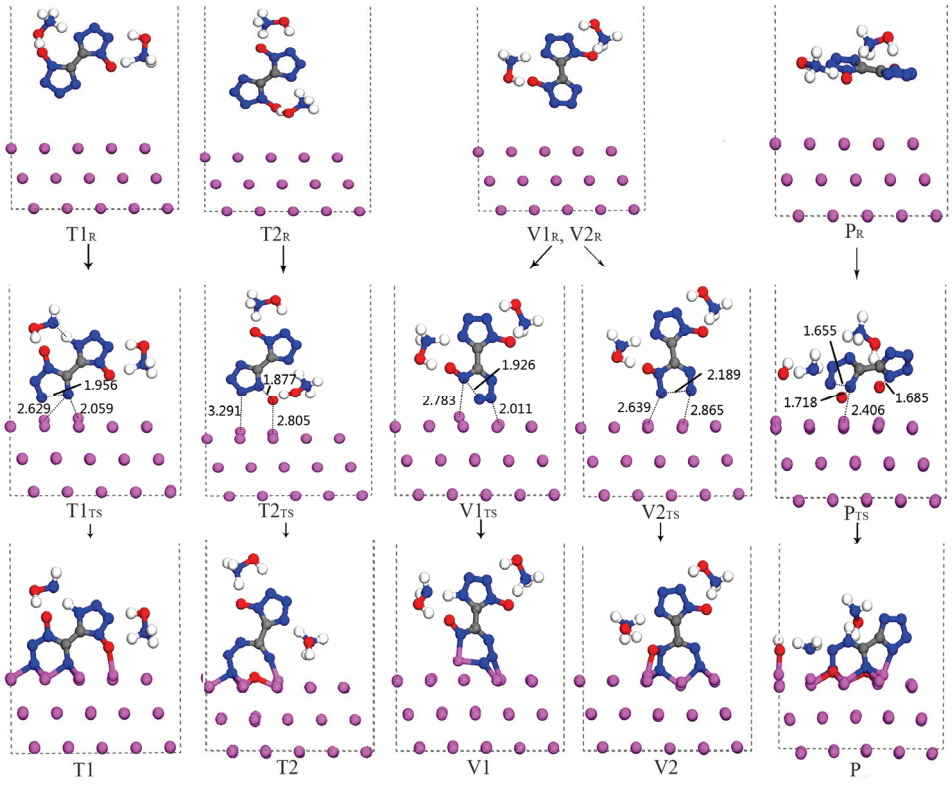

Fig. 3. Reactants, transition states and products of TKX-50 decomposition process on Al(111) surface (bond lengths are in Å).

TABLE I. Activation energy (E_a), Adsorption energy (E_{ad}) and amount of charge transfer (ΔQ) from Al surface to TKX-50 in the decomposition process; T: tilt, V: vertical, P: parallel·

Configuration	E_a / kJ·mol^{-1}	E_{ad} / kJ·mol^{-1}	$\Delta Q_{Muliken}$ / e	$\Delta Q_{Hirshfield}$ / e
T1	145.69	−239.01	1.70	0.31
T2	287.52	−383.39	2.15	0.55
V1	100.34	−113.15	1.42	0.28
V2	108.06	−222.96	1.81	0.31
P	354.10	−1334.40	4.90	1.35

As shown in Fig. 3, N_1–N_2 bond has broken in **T1** configuration, N_1 and N_2 atoms interact with Al atoms to form six Al–N bonds in length of 1.962–1.990 Å. The O'_1 atom forms an Al–O bond with Al atom, its bond length is 1.993 Å. The H atom of hydroxylammonium transferred to the N'_4 atom to form N–H bond. In **T2** configuration, the O_1 atom is detached from the tetrazole ring and adsorbed on the Al(111) surface. O_1 atom interacts with neighbouring Al atoms to form three Al–O bonds in lengths of 1.832–1.868 Å. Moreover, N_1–N_2 bond ruptures, N_1 and N_2 atoms interact with Al atoms to form four Al–N bonds totally, among these Al–N bonds, N_1 atom interacts with Al atom to form one Al–N bond with length of 1.798 Å. N_2 atom interacts with Al atoms to form three Al–N bonds in length of 1.945–1.958 Å. In **V1** configuration, the N_1–N_2 bond ruptures. N_1, N_2 and N_3 atoms interact with Al atoms to form four Al–N bonds in length of 1.883–1.952 Å. N_2–N_3 bond ruptures in the **V2** configuration. O_1, N_2 and N_3 atoms interact with Al atoms to form seven Al–X (X is O or N atom) bonds. These bonds include an Al–O bond with length of 1.993 Å and six Al–N bonds in length of 1.962–1.989 Å. In **P** configuration, O_1 and O'_1 atoms dissociate from tetrazole ring and adsorb on the Al(111) surface to form six Al–O bonds in length of 1.843–1.866 Å. Meanwhile, –OH also dissociated from the hydroxyl-ammonium and interacts with Al atom to form an OH–Al bond with length of 1.748 Å. The N_1–N_2 bond ruptures, then N_1 and N_2 atoms interact with Al atoms to form six Al–N bonds in lengths of 1.926–2.019 Å. The N'_1 atom also interacts with Al atoms to form Al–N bond with length of 1.963 Å. In all absorption configurations, due to bonding with the dissociated atoms of TKX-50, the Al atoms on the Al(111) surface deviate significantly from the original position.

As can be seen from Table I, the E_{ad} value of **V1** (–113.75 kJ/mol) is the smallest in all adsorption configurations, since there are only four Al–N bonds in **V1** configuration. The minimum of bonds are formed in all adsorption configurations. Although the atom bonding types and number of **V2** and **T1** are the same, the E_{ad} value of **T1** configuration (–239.01 kJ/mol) is slightly larger than **V2** (–222.96 kJ/mol) since the bond ruptures type of T1 is different to that of **V2** configurations. Comparing **T1** and **T2** configurations, although the number of Al–N bonds of **T2** is lower than that of **T1**, the number of Al–O bonds is higher than that of **T1**. Consequently, the E_{ad} of **T2** (–383.39 kJ/mol) is higher than that

of **T1**. The E_{ad} value of **P** is the highest (–1334.4 kJ/mol) among all configurations, since **P** includes the maximum number of Al–N and Al–O bonds.

As a whole, the tetrazole ring of TKX-50 molecule can rupture in the adsorption process. The O atoms can dissociate from tetrazole ring due to the attraction of Al atoms. Subsequently, O and N atoms of TKX-50 molecule interact with Al atoms to form Al–N and Al–O bonds. As the number of Al–X bond increase, the absolute values of adsorption energies increase as well.

Reaction mechanism

The reactants (R), transition state (TS) and products for the surface reaction of TKX-50 molecule on the Al(111) are depicted in Fig. 3. The detailed energy profile for dissociation of TKX-50 on the Al(111) surface are presented in Fig. 4. The activation energies are tabulated in Table I.

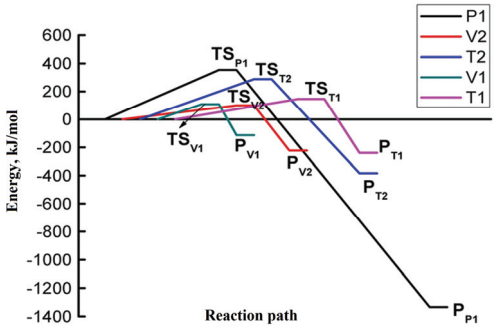

Fig. 4. Relative energy profile for TKX-50 decomposition on the Al(111) surfaces.

As can be seen from Fig. 3, N_1, N_2 and N_3 atoms interacts with several Al atoms that deviate from the Al surface in $\mathbf{V1}_{TS}$ configuration. The length of N_1–N_2 bond increases to 1.926 Å. The activation energy (E_a) of this transition state is 108.06 kJ/mol, indicating that this process takes place relatively easy. In the subsequent decomposition process, the N_1–N_2 atom distance continues to increase until N_1–N_2 bond is completely broken, N_2 and N_3 atoms are getting closer to the Al surface to form Al–N bonds. In $\mathbf{V2}_{TS}$, the N_2–N_3 bond increases to 1.936 Å since N_3 and N_4 atoms interact with Al atoms. Meanwhile, several Al atoms on Al(111) surface also deviate from the initial location. The activation energy (E_a) of $\mathbf{V2}_{TS}$ is 100.34 kJ/mol, indicating that this reaction is occurs easily. The length of N_3–N_4 bond increases to 1.956 Å in $\mathbf{T1}_{TS}$ configuration. The interaction between N_3, N_4 and Al atoms make several Al atoms deviate from the initial Al surface. The H_{1A} atom moves away from N_5 atom to N'_4 atom. In the subsequent decomposition process, the distance between N_3 and N_4 atoms continue to increase, N_3 and N_4 atoms are getting closer to the Al surface until the Al–N bond is formed. The O'_1 atom also interact with Al atom to form Al–O bond. In $\mathbf{T2}_{TS}$ configuration, the O_1 atom move away from N_1 atom. The

distance of O_1 and N_1 extends to 1.877 Å. Meanwhile, the length of N_1–N_2 bond increases to 1.820 Å. Subsequently, O_1 atom is getting closer to the Al surface until three Al–O bonds are generated. The N_1 and N_2 atoms also form Al–N bond with Al atoms. The activation energy (*E*a) of $\mathbf{T2}_{TS}$ is 287.52 kJ/mol, indicating that this reaction is hard to occur. The reaction of $\mathbf{P}_{TS}$ needs the largest activation energy (E_a = 354.10 kJ/mol), indicating that this process is difficult to occur. In $\mathbf{P}_{TS}$ configuration, several Al atoms deviate from the Al surface obviously due to their interactions with TKX-50 molecule. The distance of O_1 and N_1 increases to 1.718 Å. The distance of O'_1 and N'_1 extends to 1.685 Å, the N_2–N_3 bond length increases to 1.665 Å. The –OH moves away from the hydroxylammonium. As the reaction goes on, O_1 and O'_1 atoms separate completely from TKX-50 molecule and form Al–O bonds with Al atoms. The distance of N_1–N_2 continues to increase, N_1 and N_2 atom are getting closer to the Al surface and form Al–N bonds. –OH also interacts with Al atom and forms OH–Al bond.

By comparing with the paper on the study of TKX-50 decomposition,[7] we have found that the activation energy of N–N bonds rupture on the Al surface is reduced. For example, the activation energy of N_1–N_2 ruptures in pure TKX-50 molecule is 161.58 kJ/mol, but the activation energy of N_1–N_2 ruptures on the Al surface is 100.34 kJ/mol. In addition, the activation energy of N_2–N_3 ruptures on the Al surface (108.60 kJ/mol) is lower than that of pure TKX-50 molecule (215.99 kJ/mol). The results show that Al can obviously promote the breaking of the tetrazole ring of TKX-50.

Charge transfer

Muliken population and Hirshfeld population were used to analyze the charge transfer. Table I presents the total charge transferred from the aluminum surface to TKX-50 molecule. Although there are differences in the values of the both charges, the trend of charge is consistent. The result helped us to describe more accurately the relationship between reaction and charge transfer. In all adsorption configurations, the amount of charge transferred in **P** is the largest; **T1** has the least amount of charge transferred. Tables II and III show the Muliken atomic charges of TKX-50. By comparing the atomic charge before and after adsorption, we observed that the atomic charge varies significantly when the atom bonds with Al atom. The charges of atoms (N, O atoms) that bond to Al atom decline significantly, the charge of Al atom on the surface obviously increased. The more the number of Al–X (X is N or O atom) bonds formed in the Al surface, the more the electron transfer from Al surface to TKX-50 molecule. **T1** configuration only has four Al–N bonds, but **T2** includes one Al–O bond and six Al–N bonds. The number of charge transfer in **T2** is higher than that of **T1**. The **P** configuration forms the largest number of Al–X bonds, so its charge transfer is the most pronounced. Although there are both N–N bond rupture and the form-

ation of Al–N bond in **V1** and **V2** configurations, there is an O atom move to Al surface to form three Al–O bonds in **V2** configuration, thus the number of charge transfer in **V2** is higher than that of **V1** configurations.

TABLE II. Atomic charge (e) of TKX-50 anion in adsorption of Al(111)

Configuration	Atom											
	O_1	O'_1	N_1	N'_1	N_2	N'_2	N_3	N'_3	N_4	N'_4	C_1	C'_1
Initial	−0.55	−0.48	0.13	0.12	−0.11	−0.13	−0.11	−0.09	−0.28	−0.29	0.24	0.30
T1	−0.51	−0.56	0.16	0.07	−0.18	−0.14	−0.82	−0.07	−0.92	−0.30	0.09	0.26
T2	−1.01	−0.49	−0.77	0.11	−0.85	−0.14	−0.13	−0.09	−0.22	−0.28	0.22	0.30
V1	−0.56	−0.48	−0.31	0.12	−0.83	−0.13	−0.27	−0.07	−0.27	−0.27	0.27	0.36
V2	−0.64	−0.49	−0.12	0.11	−0.87	−0.14	−0.79	−0.09	−0.26	−0.29	0.22	0.32
P	−1.01	−1.03	−0.96	−0.42	−0.86	−0.13	−0.25	−0.11	−0.32	−0.33	0.12	0.23

TABLE III. Atomic charge (e) of hydroxylammonium anion in adsorption of Al(111)

Configuration	Atom											
	O_2	O'_2	N_5	N'_5	H_{1A}	H'_{1A}	H_{1B}	H'_{1B}	H_{1C}	H'_{1C}	H_2	H'_2
Initial	−0.60	−0.63	−0.64	−0.68	0.41	0.43	0.50	0.47	0.48	0.48	0.49	0.52
T1	−0.65	−0.58	−0.70	−0.57	0.42	0.42	0.45	0.51	0.46	0.43	0.52	0.51
T2	−0.55	−0.63	−0.54	−0.69	0.36	0.44	0.42	0.47	0.48	0.47	0.45	0.52
V1	−0.63	−0.63	−0.67	−0.68	0.40	0.44	0.46	0.46	0.46	0.48	0.50	0.53
V2	−0.58	−0.63	−0.59	−0.69	0.42	0.44	0.51	0.47	0.41	0.48	0.47	0.52
P	−1.06	−0.64	−1.12	−0.70	0.43	0.44	0.44	0.46	0.45	0.46	0.49	0.52

CONCLUSION

TKX-50 decomposes easily in the adsorption process on the Al(111) surface. The decomposition start with the ruptures of N–N and N–O bonds. Subsequently, the N and O atoms interact with Al atoms to form Al–N and Al–O bonds. As the number of Al–N and Al–O bonds increase, the absolute value of adsorption energy increases correspondingly. The decomposition of TKX-50 on Al surface is exothermic. The activation energies are in range of 100.34–354.10 kJ/mol. The charge transfer is obvious after adsorption. The atomic charge varies significantly when it bonds with Al atom. As the number of bonds increase, the charge transfer increase also.

SUPPLEMENTARY METERIAL

Additional data are available at http://www.shd.org.rs/JSCS/, or from corresponding author on request.

Acknowledgement. Y Zhao gratefully thanks the Postgraduate Innovation Project of Jiangsu Province for partial financial support.

ИЗВОД

МЕХАНИЗАМ РАЗЛАГАЊА ДИХИДРОКСИАМОНИЈУМ-5,5'-БИС(ТЕТРАЗОЛ)-1,1'-ДИОЛАТА НА **Al**(111) ПОВРШИНИ ПРЕМА ПЕРИОДИЧНОМ DFT ИЗРАЧУНАВАЊУ

YING ZHAO[1], XIAOLING XING[2], SHENGXIANG ZHAO[2] и XUEHAI JU[1]

[1]School of Chemical Engineering, Nanjing University of Science and Technology, Nanjing 210094, P. R. China и [2]Xi'an Modern Chemistry Research Institute, Xi'an 710065, P. R. China

Методе апроксимација уопштеног градијента (GGA) из теорије функционала густине (DFT) коришћене су за истраживање разлагања ТКХ-50 молекула на Al(111) површини. За израчунавање је коришћен плочасти модел Al суперћелија и периодични гранични услови. Проучавано је пет врста конфигурација адсорбовања ТКХ-50 на Al површини. ТКХ-50 је адсорбован на Al површини уз формирање N–Al, O–Al и OH–Al веза. Енергије адсорпције су у распону од −113,15 до −1334,40 kJ/mol. Активационе енергије свих конфигурација су у распону 100,34–354,10 kJ/mol. Раскидање N_1–N_2 у **V1** и раскидање N_2–N_3 у **V2** се лако дешава. Активационе енергије ових двају веза (100,34 и 108,06 kJ/mol, редом) су мање него у чистом ТКХ-50 (161,58 и 215,99 kJ/mol). Al атоми олакшавају раскидање тетразолског прстена у ТКХ-50. Количина преноса електрона са Al атома на ТКХ-50 је у распону од 1,42–4,90 e.

(Примљено 28. августа, ревидирано 1. новембра, прихваћено 27. новембра 2019)

REFERENCES

1. M. Celina, L. Minier, R. Assink, *Thermochim. Acta* **384** (2002) 343 (https://doi.org/10.1016/S0040-6031(01)00793-6)
2. M. Gaurav, P. A. Ramakrishna, *Combust. Flame* **166** (2016) 203 (https://doi.org/10.1016/j.combustflame.2016.01.019)
3. A. Dokhan, E. W. Price, J. M. Seitzman, R. K. Sigman, *Proc. Combust. Inst.* **29** (2002) 2939 (https://doi.org/10.1016/S1540-7489(02)80359-5)
4. S. Verma, P. A. Ramakrishna, *J. Propul. Power* **29** (2013) 1200 (https://doi.org/10.2514/1.B34772)
5. N. Fischer, D. Fischer, T. M. Klapotke, D. G. Piercey, J. Stierstorfer, *J. Mater. Chem.* **22** (2012) 20418 (https://doi.org/10.1039/c2jm33646d)
6. H. F. Huang, Y. M. Shi, J. Yang, *J. Therm. Anal. Calorim.* **121** (2015) 705 (https://doi.org/10.1007/s10973-015-4472-9)
7. Q. An, W. G. Liu, W. A. Goddard, T. Cheng, S. V. Zybin, H. Xiao, *J. Phys. Chem., C* **118** (2014) 27175 (https://doi.org/10.1021/jp509582x)
8. B. Yuan, Z. J. Yu, E. R. Bernstein, *J. Phys. Chem., A* **142** (2015) 10247 (https://doi.org/10.1063/1.4916111)
9. J. F. Wang, S. S. Chen, S. H. Jin, R. Shi, Z. F. Yu, Q. Su, X. Ma, C. Y. Zhang, Q. H. Shu, *J. Therm. Anal. Calorim.* **134** (2018) 2049 (https://doi.org/10.1007/s10973-018-7820-8)
10. S. Q. Zhou, Y. Y. Wu, S. Y. Xu, F. Q. Zhao, X. H. Ju, *Can. J. Chem.* **84** (2000) 705 (https://doi.org/10.1139/cjc-2015-0278)
11. J. X. Guo, L. Guan, F. Bian, Q. X. Zhao, Y. L. Wang, B. T. Liu, *Surface Interf. Anal.* **43** (2011) 940 (https://doi.org/10.1002/sia.3665)
12. Acceryls Inc., *Material Studio 7.0.*, Acceryls Inc, San Diego, CA, 2013
13. M. R. Elahifard, M. P. Jigato, J. W. Niemantsverdriet, *Surface Interf. Anal.* **13** (2012) 89 (https://doi.org/10.1002/cphc.201100733)
14. A. Govender, D. C. Ferre, J. W. Niemantsverdriet, *Chem. Phys. Chem.* **13** (2012) 1591 (https://doi.org/10.1002/cphc.201100733)

15. V. A. Ranea, T. J. Strathmann, J. R. Shapley, W. F. Schneider, *Phys. Chem.* **3** (2011) 898 (https://doi.org/10.1002/cctc.201000398)
16. R. Q. Liu, *Comput. Theor. Chem.* **1019** (2013) 141 (https://doi.org/10.1016/j.comptc.2013.07.009)
17. X. Wang, P. Qian. K. H. Song, C. Zhang, J. Dong. *Comput. Theor. Chem.* **1025** (2013) 16 (https://doi.org/10.1016/j.comptc.2013.09.025)
18. M. Rouhani. B, Al, Ga, Si and Ge doped graphene, *J. Mol. Struct.* **1181** (2019) 518 (https://doi.org/10.1016/j.molstruc.2019.01.006)
19. N. Yildirim, N. Demir, G. Alpaslan, B. Boyacioglu, M. Yildiz, H. Unver, *J Serb. Chem. Soc.* **83** (2018) 6 (https://doi.org/10.2298/JSC171001009Y)
20. J. Z. Yu, F. Q. Zhao, S. Y. Xu, X. H. Ju, *J. Serb. Chem. Soc.* **82** (2017) 163 (https://doi.org/10.2298/JSC160331084Y)
21. M. Rafique, Y. S. M. Hassana, *J. Mol. Struct.* **1142** (2017) 11 (https://doi.org/10.1016/j.molstruc.2017.04.045)
22. E. Escamilla-Roa, V. Timón, A. Hernández-Laguna, *J. Mol. Struct.* **981** (2012) 59 (https://doi.org/10.1016/j.comptc.2011.11.046)
23. C. J. Pickard, M. C. Payne, *Phys. Rev., B* **62** (2000) 4383 (https://doi.org/10.1103/PhysRevB.62.4383)
24. J. P. Perdew, W. Yue, *Phys. Rev., B* **33** (1986) 8800 (https://doi.org/10.1103/PhysRevB.33.8800)
25. M. A. L. Marques, J. Vidal, M. J. T. Oliveira, L. Reining, S. Botti, *Phys. Rev., B* **83** (2011) 035119 (https://doi.org/10.1103/PhysRevB.83.035119)
26. A. Mokhtari, A. Ribeiro, *IEEE Trans. Signal Process.* **62** (2014) 6089 (https://doi.org/10.1109/TSP.2014.2357775)
27. C. C. Ye, F. Q. Zhao, S. Y. Xu, X. H. Ju, *J. Mol. Model.* **19** (2013) 4459 (https://doi.org/10.1007/s00894-013-1942-5)
28. C.C. Ye, Q. An, S.Y. Xu, X.H. Ju. *Surface Interf. Anal.* **49** (2017) 441 (https://doi.org/10.1002/sia.6177)
29. D. Shahabi, H. Tavakol, *Comput. Theor. Chem.* **1127** (2018) 8 (https://doi.org/10.1016/j.comptc.2018.02.001).